International Journal of Power Electronics and Drive System (IJPEDS)
Vol. 17, No. 3, September 2026, pp. 1822∼1830
ISSN: 2088-8694, DOI: 10.11591/ijpeds.v17.i3.pp1822-1830 ❒ 1822

Comparative simulation of fractional-order PD sliding mode and fuzzy logic controllers for a second-order discrete-time nonlinear system

Ahmed Bennaoui[1], Salah Benzian[1], Hamza Sulimani[2], Aissa Ameur[3]
[1]Institute of Sciences, University Center Aflou El Cherif Bouchoucha, Aflou, Algeria
[2]Department of Computer and Network Engineering, College of Computing, Umm Al-Qura University, Makkah, Saudi Arabia
[3]Faculty of Technology, University of Amar Telidji, Laghouat, Algeria

Article Info

Article history:

Received Oct 20, 2025
Revised May 15, 2026
Accepted Jul 8, 2026

Keywords:

Fractional-order control
Fuzzy logic control
Nonlinear systems
Power electronics and drive systems
Sliding mode control

ABSTRACT

Tight output regulation in power converters and electric drive systems requires a control strategy that simultaneously minimizes tracking error and maintains smooth actuation—two objectives that are intrinsically in tension for nonlinear, parameter-varying plants. Despite the widespread deployment of fractional-order PD sliding mode control (FOPD-SMC) and Mamdani fuzzy logic control (FLC) in this domain, no prior study has placed them in a direct, metric-identical comparison on a common plant. The present work closes this gap by implementing both controllers on the same second-order discrete-time nonlinear plant—representative of DC-DC converter output dynamics and motor-drive input-output behavior and evaluating them under a composite reference that combines sinusoidally-modulated ramps with step transitions, scored by the integral of squared error (ISE) and integral of absolute error (IAE). FOPD-SMC achieves ISE$=1.639\times10^{-2}$ and IAE$=3.345\times10^{-2}$, outperforming FLC by 87.6% and 50.4%, respectively; the advantage originates from the non-integer memory embedded in the sliding surface via the Grünwald–Letnikov operator and from the explicit decomposition of the control law into nominal-tracking and robustness components. FLC, conversely, produces a chattering-free, continuously varying control signal a structural consequence of smooth Gaussian membership functions and linguistic rule aggregation, at the cost of a mean absolute tracking error twice that of FOPD-SMC. These findings establish a quantitative selection criterion: FOPD-SMC is recommended when tight voltage or current regulation is the primary objective, while FLC is preferred where smooth torque delivery and reduced actuator stress outweigh marginal gains in tracking accuracy.

Corresponding Author:

Ahmed Bennaoui
Institute of Sciences, University Center Aflou El Cherif Bouchoucha
Aflou 03001, Algeria
Email: a.bennaoui@cu-aflou.edu.dz

1. INTRODUCTION

The proliferation of grid-connected inverters, DC–DC switched-mode power supplies, and variable-speed electric drives has placed increasingly stringent demands on closed-loop regulation: tight voltage and current control in converter stages, precise speed tracking with fast disturbance rejection in drive systems, and, in both cases, a control signal that does not induce excessive switching stress or mechanical wear. Meeting these objectives simultaneously is non-trivial, because power electronic plants are inherently nonlinear-switching phenomena, magnetic saturation, and duty-cycle-dependent operating points generate behaviors that linear time-invariant models cannot reproduce—and because precision and smoothness are intrinsically competing requirements: a more aggressive law reduces tracking error while typically exciting higher-frequency actuation [1], [2]. Fixed-gain proportional-integral-derivative (PID) regulators, despite their industrial prevalence, are especially sensitive to this tension: their parameters are tuned at a nominal operating point and degrade under nonlinear excursions or parameter drift [3], making advanced model-flexible strategies necessary for demanding converter and drive applications.

Two paradigms have attracted sustained research attention in this context. Sliding mode control (SMC) achieves robust disturbance rejection by confining the system trajectory to a designer-chosen manifold; beyond that manifold, matched perturbations are structurally decoupled from the closed-loop output [1], [2]. Finite-time convergence extensions-Terminal SMC [4], nonsingular fast TSMC [5], and global terminal SMC [6]-tighten this guarantee from asymptotic to finite-time. Incorporating fractional-order calculus [7] into the sliding surface has proved a particularly productive direction: Pisano *et al.* [8] formulated a rigorous sliding-mode regulator for fractional-order dynamics; Matignon [9] established the underlying stability theory; and Yin *et al.* [10], Xue *et al.* [11], and Monje *et al.* [12] demonstrated that replacing the classical integer-order derivative with a non-integer memory operator yields measurably better tracking. This fractional-order PD sliding mode control (FOPD-SMC) approach has since been extended to power electronics, where Wang *et al.* [13] and Bennaoui *et al.* [14] reported improved regulation on boost and dual-active-bridge converters. Fuzzy logic control (FLC), introduced by Zadeh [15] and Mamdani [16] and later systematized by Lee [17], Jang [18], Ross [19], Passino and Yurkovich [20], and Feng [21], offers a structurally different approach: by encoding expert knowledge as linguistic if–then rules rather than an analytical plant model, it inherently smooths the control action across the entire operating range. This advantage has been confirmed across diverse application domains, including hybrid power systems [22], induction motor drives [23], power system stabilizers [24], and doubly-fed induction generator protection [25]. Building on these directions, Tiwary *et al.* [26] proposed a super-twisting sliding-mode regulator for dual-active-bridge converters, Abdelrahem *et al.* [27] applied a predictive sliding-mode scheme to wind-turbine generators, and Zhao and Guo [28] developed PID design guidelines for nonlinear systems.

Despite the breadth of this body of work, a critical question remains unanswered: when FOPD-SMC and FLC are tested on the same plant and driven by the same reference, how large is the quantitative trade-off between their tracking precision and their actuator smoothness? Existing studies invariably evaluate each paradigm in isolation on application-specific hardware, so any cross-paradigm inference is confounded by differences in plant topology, operating conditions, and evaluation criteria. Practitioners designing a voltage regulator or drive controller therefore lack a numerically grounded reference from which to read off the accuracy cost of choosing FLC over FOPD-SMC, or the smoothness penalty of the reverse selection. To address this gap, the present work makes three contributions: i) Both controllers are implemented on the same second-order discrete-time nonlinear plant whose ARX structure emulates the input–output dynamics of DC–DC converter filters and electric motor drives; ii) Both are evaluated under a composite reference combining sinusoidally-modulated ramps with step transitions—spanning the speed-ramp and load-step profiles of real drive operation—and scored with identical ISE and IAE metrics; and iii) The measured precision-versus-smoothness trade-off is translated into quantitative, evidence-based selection guidelines applicable to voltage regulators, DC–DC converters, and variable-speed drive systems.

2. METHOD

2.1. Research design

The study is a controlled simulation experiment that isolates each control law by holding every other variable fixed. The workflow is: i) Define a second-order discrete-time nonlinear plant representative of converter/drive dynamics; ii) Design FOPD-SMC and FLC with documented parameters and stability properties; iii) Drive both closed loops with an identical composite reference; and iv) Evaluate tracking accuracy and control smoothness via ISE and IAE. All simulations were performed in Python 3.10 with NumPy and scikit-fuzzy.

2.2. Plant model

The controlled plant is a second-order discrete-time system described by (1).

$$y[i] = 0.7\,y[i-1] + 0.3\,u[i-1] + 0.05\,u[i-2] \tag{1}$$

This second-order autoregressive with eXogenous inputs (ARX) structure captures two key dynamic characteristics common to power electronic and drive system plants: i) The autoregressive coefficient 0.7 on $y[i-1]$ represents the dominant energy-storage pole dynamics typical of a direct current (DC)–DC converter output filter (LC network) or a motor winding with a significant electrical time constant; and ii) The two input terms $0.3\,u[i-1] + 0.05\,u[i-2]$ model a delayed, distributed input-to-output response analogous to the combined effects of pulse width modulation (PWM) switching delays and electromagnetic inertia in electric drive systems [1], [11]. The presence of a second-order delayed-input term renders the control design non-trivial, as any controller must account for the additional phase lag introduced by $u[i-2]$. This benchmark structure follows the approach of prior comparative controller evaluation studies [10], [13] and provides a common, reproducible basis for assessing control law performance independent of hardware-specific converter topologies. The composite reference signal used in all closed-loop experiments consists of sinusoidally-modulated triangular ramps concatenated with a $\{0, 5, 0\}$ square-wave segment, emulating the speed-ramp profiles and load-step disturbances encountered in real drive operation.

2.3. Fractional-order PD sliding mode controller

The FOPD-SMC replaces the classical integer-order error derivative in the sliding surface with a Grünwald–Letnikov (GL) operator of non-integer order α, injecting a weighted history of past error values into the surface computation and thereby enriching the controller's anticipatory capability [10], [11], [13]. The tracking error is (2).

$$e[i] = y[i] - r[i+1] \tag{2}$$

The fractional-order sliding surface is as (3).

$$s[i] = e[i] + \lambda D^{\alpha} e[i] \tag{3}$$

Where $\lambda = 2.0$ and $\alpha = 0.5$. The GL recursion truncates the infinite binomial series at M past samples, producing the causal finite-memory approximation used at each step i.

$$D^{\alpha} e[i] \approx \frac{1}{h^{\alpha}} \sum_{j=0}^{M} (-1)^j \binom{\alpha}{j} e[i-j] \tag{4}$$

The control law includes equivalent control:

$$u_{eq}[i] = -\frac{p}{q} \tag{5}$$

where:

$$p = (1+\lambda)a + \lambda F_{i+1}, \quad a = 0.7y[i] + 0.05u[i-1] - r[i+2] \tag{6}$$

$$q = (1+\lambda)0.3 \tag{7}$$

$$F_{i+1} = \sum_{k=1}^{\min(M,i+1)} (-1)^k \binom{\alpha}{k} e[i+1-k], \quad M = 20 \tag{8}$$

and switching control (9).

$$u_{sw}[i] = -k_{sw}\,\mathrm{sign}(s[i]), \quad k_{sw} = 0.1 \tag{9}$$

The total control signal is (10).

$$u[i] = u_{eq}[i] + u_{sw}[i] \tag{10}$$

Closed-loop stability is verified through the quadratic Lyapunov candidate (11).

$$V[i] = \frac{1}{2}s[i]^2 \tag{11}$$

The equivalent term u_{eq} is derived to annihilate the plant dynamics and set $s[i+1] = 0$ on the nominal trajectory; the discontinuous term u_{sw} then enforces $\Delta V[i] < 0$ for all $s[i] \neq 0$, so the surface is globally attractive. The value $k_{sw} = 0.1$ was selected to bound the worst-case residual perturbation while holding the discontinuous amplitude—and the resulting chattering—within acceptable limits [1], [2].

2.4. Fuzzy logic controller

The FLC adopts the Mamdani incremental architecture [16], [17]: the instantaneous tracking error $e[i] = y[i] - r[i+1]$ and its one-step difference $\Delta e[i] = e[i] - e[i-1]$ serve as linguistic inputs, while $\Delta u[i]$ is the inferred output increment. Each input is encoded by three Gaussian membership functions as show in Figures 1(a) and 1(b) and the output by five triangular labels as shows in Figure 1(c). The nine-rule base as shown in Table 1 embeds the heuristic that larger errors or faster error growth should trigger proportionally larger corrective increments. The crisp control signal is reconstructed as (12).

$$u[i] = u[i-1] + \text{Gain} \cdot \Delta u[i], \quad \text{Gain} = 1.8. \tag{12}$$

Membership widths ($\sigma = 6$ on $[-10, 10]$ for inputs; triangular partitions on $[-15, 15]$ for the output) distribute the linguistic coverage evenly across the expected operating range. Rule firing strengths are aggregated by min-max composition [16], [19], [20] and the crisp increment is recovered by centre-of-gravity defuzzification. This integrating structure-accumulated control rather than direct output-is a standard strategy in FLC-based drive and power-system compensation [22], [23], [25].

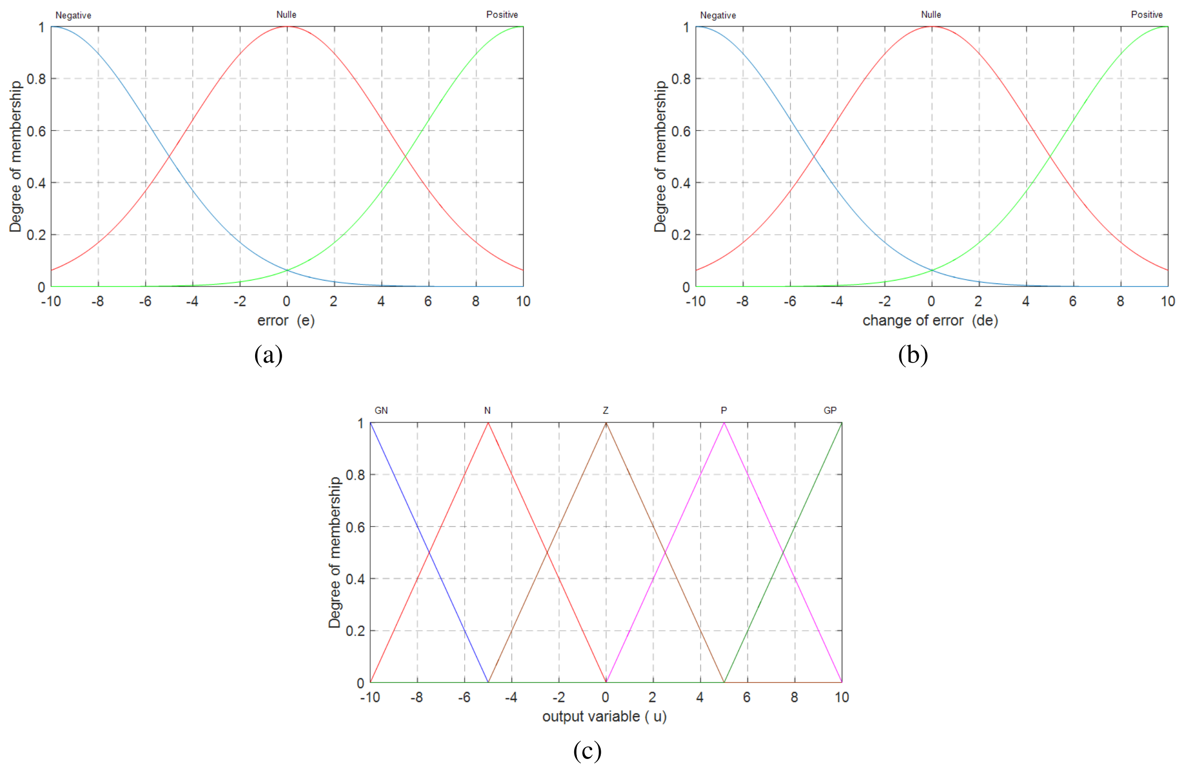

(a) (b)

(c)

Figure 1. Membership functions of the Mamdani FLC: (a) error, (b) error derivative, and (c) change in control signal

Table 1. FLC rule base

$e\backslash\Delta e$	Negative	Zero	Positive
Negative	GP	P	Z
Zero	P	Z	N
Positive	Z	N	GN

Notes: GP: great positive, P: positive, Z: zero
N: negative, GN: great negative

2.5. Implementation and software tools

Both controllers were implemented in Python 3.10 using NumPy and scikit-fuzzy, in strictly separate closed loops sharing only the plant and reference. At each step i, the FOPD-SMC evaluates the Grünwald–Letnikov derivative (4) (memory depth $M = 20$), computes the sliding surface (3), and applies the total control law (10). FLC fuzzifies $e[i]$ and $\Delta e[i]$, evaluates the nine rules via Mamdani min–max inference, and applies the defuzzified increment through (12). ISE and IAE are computed from $i = 2$ onward to exclude initialization transients. This study involves only numerical simulation and requires no ethical approvals.

3. RESULTS AND DISCUSSION

3.1. Simulation conditions

Both controllers were simulated on plant (1) for $N = 600$ samples ($T_s = 1$, zero initial conditions) and driven by the same composite reference (sinusoidally-modulated ramp followed by a $\{0, 5, 0\}$ square-wave segment). Tracking performance was quantified by (13).

$$\text{ISE} = \frac{1}{N-2}\sum_{i=2}^{N-1} e[i]^2, \qquad \text{IAE} = \frac{1}{N-2}\sum_{i=2}^{N-1} |e[i]| \tag{13}$$

Where ISE assigns quadratic weight to transient excursions and IAE measures the mean absolute deviation over the full simulation horizon.

3.2. Presentation of results

Table 2 reports quantitative performance under identical conditions. FOPD-SMC achieves an ISE of 1.639×10^{-2} and an IAE of 3.345×10^{-2}, while FLC yields an ISE of 1.323×10^{-1} and an IAE of 6.742×10^{-2}. Figure 2 presents on same time axis, Figure 2(a) show reference and both outputs, Figure 2(b) show tracking errors, and Figure 2(c) show control signals. Figure 3 shows FOPD-SMC sliding surface $s[i]$.

3.3. Analysis and interpretation

The measured reductions of 87.6% in ISE and 50.4% in IAE establish a consistent and reproducible tracking advantage for FOPD-SMC over FLC. Translating the IAE values into per-sample terms: FOPD-SMC averages an absolute deviation of ≈ 0.033 per sample against ≈ 0.067 for FLC, so FLC's typical pointwise error is double that of its fractional-order counterpart across the entire 600-sample run. The ISE ratio of 8.07 signals that FLC generates pronounced transient overshoots at reference step transitions—spikes that the quadratic metric amplifies disproportionately—as confirmed by the delayed output response visible in Figure 2(a), where FLC peak deviations reach 3–4 times the FOPD-SMC level during abrupt changes.

Two structural properties account for FOPD-SMC's superior performance. First, setting $\alpha = 0.5$ in (3) gives $s[i]$ access to a decaying-weight history of past errors: the GL operator assigns larger coefficients to recent samples and progressively smaller ones to older samples, so the surface responds to error trends that a purely instantaneous derivative would miss. Second, the control signal is constructed in two functionally separate parts—u_{eq} handles the nominal plant trajectory while u_{sw} provides a hard robustness margin against model residuals—so the two requirements never compete. Figure 3 provides direct evidence of this design: $s[i]$ falls sharply to zero within the first few dozen samples and subsequently remains confined to a narrow corridor, confirming that the controller reaches and sustains sliding-mode operation throughout the full run. The precision gain carries a visible cost in Figure 2(b): the hard relay nonlinearity $\text{sign}(\cdot)$ in u_{sw} forces rapid amplitude transitions around the sliding manifold, exciting unmodeled high-frequency plant dynamics and producing the characteristic oscillatory artifact that must be addressed in hardware realizations through boundary-layer replacement or higher-order SMC schemes [1], [2]. FLC, by contrast, maps its inputs through smooth Gaussian functions and aggregates nine rules by min-max composition, so the control increment varies continuously with the error state; this structural smoothness eliminates rapid switching at the cost of the 3–4× larger peak deviations observed in Figure 2(b) during abrupt reference changes. These observations make the precision-versus-smoothness trade-off directly measurable on a common benchmark rather than inferred across heterogeneous application studies.

Table 2. Performance comparison

Controller	ISE	IAE
FOPD-SMC	1.639×10^{-2}	3.345×10^{-2}
FLC	1.323×10^{-1}	6.742×10^{-2}

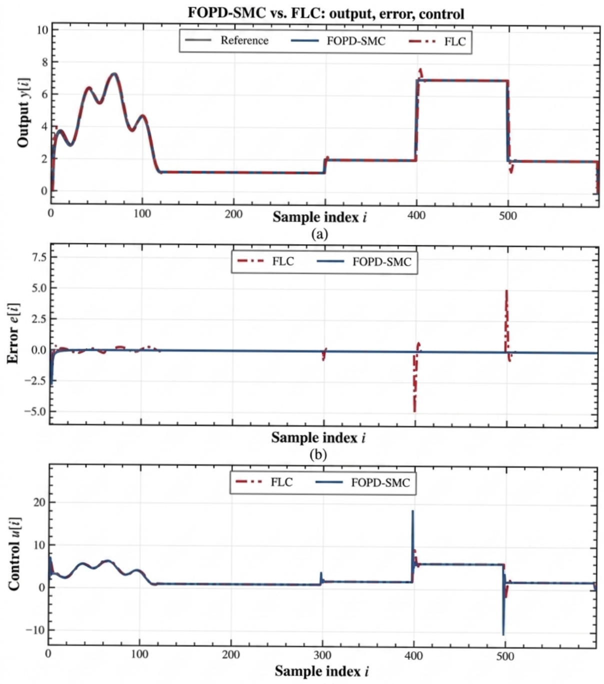

Figure 2. FOPD-SMC versus FLC on a common time axis: (a) reference and closed-loop outputs, (b) tracking errors, and (c) control signals

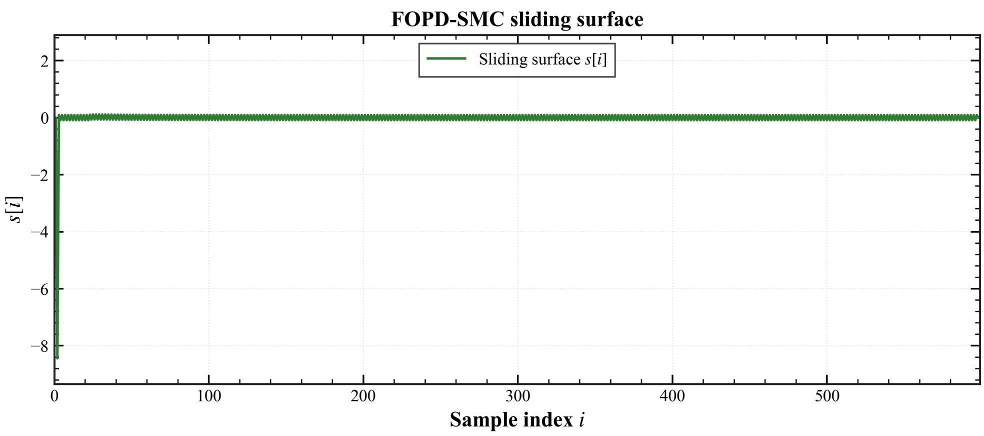

Figure 3. FOPD-SMC sliding surface $s[i]$, confirming that the sliding mode is reached and maintained throughout the simulation horizon

4. CONCLUSION

This paper presented a controlled, cross-paradigm benchmarking of FOPD-SMC and Mamdani FLC on a common second-order discrete-time nonlinear plant under identical reference, initial conditions, and performance metrics. By removing the application-specific confounds present in prior studies—which typically evaluate a single controller on one particular converter or drive topology—the experiment yields the first directly comparable ISE/IAE measurements for these two control families under a common evaluation protocol.

FOPD-SMC outperforms FLC with ISE $= 1.639 \times 10^{-2}$ and IAE $= 3.345 \times 10^{-2}$, corresponding to reductions of 87.6% and 50.4%, respectively, over FLC (ISE $= 1.323 \times 10^{-1}$, IAE $= 6.742 \times 10^{-2}$). The performance advantage stems from two cooperating mechanisms: the Grünwald–Letnikov fractional-order derivative embedded in the sliding surface introduces an error-history memory that anticipates reference changes earlier than integer-order designs, while explicit decomposition of the control law into equivalent and switching components ensures simultaneous nominal tracking and robustness to plant uncertainty. FLC, although 8.07× less precise in ISE, inherently suppresses chattering through smooth rule-based inference, rendering it the preferred option in applications where actuator smoothness and reduced mechanical wear are paramount.

The study is subject to three main limitations: only a single second-order plant structure is evaluated; measurement noise, actuator saturation, and parametric uncertainty are not modeled; and the computational burden of the Grünwald–Letnikov recursion relative to FLC inference is not formally profiled. Future work will extend the benchmark to experimental validation on a DC–DC converter and a motor-drive testbed, investigate a hybrid architecture in which FLC adaptively tunes the FOPD-SMC parameters (λ, k_{sw}) in real time to combine high precision with chattering-free actuation, and assess performance on higher-order plants and multi-input multi-output drive configurations.

ACKNOWLEDGEMENTS

The authors extend their appreciation to Umm Al-Qura University, Saudi Arabia for funding this research work through grant number: 26UQU4320283GSSR02.

FUNDING INFORMATION

Funded by Umm Al-Qura University, Saudi Arabia, grant number: 26UQU4320283GSSR02.

AUTHOR CONTRIBUTIONS STATEMENT

This journal uses the Contributor Roles Taxonomy (CRediT) to recognize individual author contributions, reduce authorship disputes, and facilitate collaboration.

Name of Author	C	M	So	Va	Fo	I	R	D	O	E	Vi	Su	P	Fu
Ahmed Bennaoui	✓	✓	✓		✓	✓			✓					
Salah Benzian		✓			✓					✓				
Hamza Sulimani		✓	✓	✓						✓				
Aissa Ameur			✓		✓					✓				

C	: **C**onceptualization	I	: **I**nvestigation	Vi	: **Vi**sualization
M	: **M**ethodology	R	: **R**esources	Su	: **Su**pervision
So	: **So**ftware	D	: **D**ata Curation	P	: **P**roject Administration
Va	: **Va**lidation	O	: Writing - **O**riginal Draft	Fu	: **Fu**nding Acquisition
Fo	: **Fo**rmal Analysis	E	: Writing - Review & **E**diting		

CONFLICT OF INTEREST STATEMENT

The authors declare no conflict of interest.

DATA AVAILABILITY

Data are available from the corresponding author upon reasonable request.

REFERENCES

[1] V. I. Utkin, "Sliding mode control design principles and applications to electric drives," *IEEE Transactions on Industrial Electronics*, vol. 40, no. 1, pp. 23–36, Feb. 1993, doi: 10.1109/41.184818.

[2] C. Edwards and S. K. Spurgeon, *Sliding mode control: theory and applications. London*. London, UK: Taylor & Francis, 1998.

[3] J. Viola, L. Angel, and J. M. Design and robust performance evaluation of a fractional order PID controller applied to a DC motor," *IEEE/CAA Journal of Automatica Sinica*, vol. 4, no. 2, pp. 304–314, Apr. 2017, doi: 10.1109/JAS.2017.7510535.

[4] X. Yu and M. Zhihong, Fast terminal sliding-mode control design for nonlinear dynamical systems," *IEEE Transactions on Circuits and Systems I: Fundamental Theory and Applications*, vol. 49, no. 2, pp. 261–264, 2002, doi: 10.1109/81.983876.

[5] L. Yang and J. Yang, "Nonsingular fast terminal sliding-mode control for nonlinear dynamical systems," *International Journal of Robust and Nonlinear Control*, vol. 21, no. 16, pp. 1865–1879, Nov. 2011, doi: 10.1002/rnc.1666.

[6] S. Yu, X. Yu, and M. Zhihong, "Robust global terminal sliding mode control of siso nonlinear uncertain systems," *Proceedings of the 39th IEEE Conference on Decision and Control (Cat. No.00CH37187)*, IEEE, pp. 2198–2203. doi: 10.1109/CDC.2000.914122.

[7] I. Podlubny, "Fractional differential equations," in *Mathematics in Science and Engineering*, San Diego, CA, USA: Academic Press, 1999.

[8] A. Pisano, M. R. Rapaić, Z. D. Jeličić, and E. Usai, "Sliding mode control approaches to the robust regulation of linear multivariable fractional-order dynamics," *International Journal of Robust and Nonlinear Control* , vol. 20, no. 18, pp. 2045–2056, Dec. 2010, doi: 10.1002/rnc.1565.

[9] D. Matignon, "Stability results for fractional differential equations with applications to control processing," *Computational engineering in systems applications*, pp. 963–968, 1996.

[10] C. Yin, Y. Chen, and S. Zhong, "Fractional-order sliding mode based extremum seeking control of a class of nonlinear systems," *Automatica*, vol. 50, no. 12, pp. 3173–3181, Dec. 2014, doi: 10.1016/j.automatica.2014.10.027.

[11] D. Xue, C. Zhao, and Y. Chen, "Fractional order PID control of a DC-motor with elastic shaft: a case study," in *2006 American Control Conference*, IEEE, 2006, p. 6 pp. doi: 10.1109/ACC.2006.1657207.

[12] C. A. Monje, Y. Chen, B. M. Vinagre, D. Xue, and V. Feliu, *Fractional-order systems and controls*. in Advances in Industrial Control. London: Springer London, 2010. doi: 10.1007/978-1-84996-335-0.

[13] J. Wang, D. Xu, H. Zhou, and T. Zhou, "Adaptive fractional order sliding mode control for boost converter in the battery/supercapacitor HESS," *PLOS ONE*, vol. 13, no. 4, p. e0196501, Apr. 2018, doi: 10.1371/journal.pone.0196501.

[14] A. Bennaoui, S. Benzian, I. N. Alsolbi, and A. Ameur, "Comparative analysis of fractional-order sliding mode and pole placement control for robotic manipulator," *Indonesian Journal of Electrical Engineering and Computer Science*, vol. 41, no. 1, p. 90, Jan. 2026, doi: 10.11591/ijeecs.v41.i1.pp90-98.

[15] L. A. Zadeh, "Fuzzy sets," *Information and Control*, vol. 8, no. 3, pp. 338–353, Jun. 1965, doi: 10.1016/S0019-9958(65)90241-X.

[16] E. H. Mamdani, "Application of fuzzy algorithms for control of simple dynamic plant," *Proceedings of the Institution of Electrical Engineers*, vol. 121, no. 12, p. 1585, 1974, doi: 10.1049/piee.1974.0328.

[17] C. C. Lee, "Fuzzy logic in control systems: fuzzy logic controller. I," *IEEE Transactions on Systems, Man, and Cybernetics*, vol. 20, no. 2, pp. 404–418, 1990, doi: 10.1109/21.52551.

[18] J.-S. R. Jang, "ANFIS: adaptive-network-based fuzzy inference system," *IEEE Transactions on Systems, Man, and Cybernetics*, vol. 23, no. 3, pp. 665–685, 1993, doi: 10.1109/21.256541.

[19] T. J. Ross, *Fuzzy logic with engineering applications*, 4th ed. Chichester, UK: John Wiley & Sons, 2017.

[20] K. M. Passino and S. Yurkovich, *Fuzzy control*. Menlo Park, CA, USA: Addison-Wesley, 1998.

[21] G. Feng, "A survey on analysis and design of model-based fuzzy control systems," *IEEE Transactions on Fuzzy Systems*, vol. 14, no. 5, pp. 676–697, Oct. 2006, doi: 10.1109/TFUZZ.2006.883415.

[22] K. N. Khallouf, H. Benbouhenni, and N. Bizon, "Boosting energy quality in hybrid power systems through fractional-order adaptive fuzzy logic–based direct power control of SAPF," *Algorithms*, vol. 19, no. 5, p. 418, May 2026, doi: 10.3390/a19050418.

[23] Y.-S. Lai and J.-C. Lin, "New hybrid fuzzy controller for direct torque control induction motor drives," *IEEE Transactions on Power Electronics*, vol. 18, no. 5, pp. 1211–1219, Sep. 2003, doi: 10.1109/TPEL.2003.816193.

[24] L. Chaib, A. Choucha, and S. Arif, "Optimal design and tuning of novel fractional order pid power system stabilizer using a new metaheuristic bat algorithm," *Ain Shams Engineering Journal*, vol. 8, no. 2, pp. 113–125, Jun. 2017, doi: 10.1016/j.asej.2015.08.003.

[25] O. Noureldeen and I. Hamdan, "A novel controllable crowbar based on fault type protection technique for DFIG wind energy conversion system using adaptive neuro-fuzzy inference system," *Protection and Control of Modern Power Systems*, vol. 3, no. 1, p. 35, Dec. 2018, doi: 10.1186/s41601-018-0106-0.

[26] N. Tiwary, V. Naik N, A. K. Panda, A. Narendra, and R. K. Lenka, "A robust voltage control of DAB converter with super-twisting sliding mode approach," *IEEE Journal of Emerging and Selected Topics in Industrial Electronics*, vol. 4, no. 1, pp. 288–298, Jan. 2023, doi: 10.1109/JESTIE.2022.3227007.

[27] M. Abdelrahem, C. Hackl, and R. Kennel, "Robust predictive control scheme for permanent-magnet synchronous generators based modern wind turbines," *Electronics*, vol. 10, no. 13, p. 1596, Jul. 2021, doi: 10.3390/electronics10131596.

[28] C. Zhao and L. Guo, "PID controller design for second order nonlinear uncertain systems," *Science China Information Sciences*, vol. 60, no. 2, p. 022201, Feb. 2017, doi: 10.1007/s11432-016-0879-3.

BIOGRAPHIES OF AUTHORS

Ahmed Bennaoui received his B.Sc. in electronics engineering from the University of Mohamed Boudiaf (M'sila, 2011), M.Sc. degrees in electrical engineering (advanced automation) from the University of Ziane Achour (Djelfa, 2012 and 2016), and a Ph.D. in electrical engineering (intelligent control and automation, 2024) from the University of Amar Telidji (Laghouat), Algeria. He is currently with the Institute of Sciences, University Center Aflou El Cherif Bouchoucha. His research interests include nonlinear dynamics, fuzzy logic control, power system control, and optimization techniques. In this study, he led the design and simulation of the FOPD-SMC and the analysis of control strategies for nonlinear systems. He can be contacted at email: a.bennaoui@cu-aflou.edu.dz.

Salah Benzian received his B.Sc. from the University of M'hamed Bougara, Boumerdes, Algeria, his M.Sc. from the University of Ziane Achour, Djelfa, Algeria, and his Ph.D. from the University of Amar Telidji, Laghouat, Algeria. He is currently with the Institute of Sciences, University Center Aflou El Cherif Bouchoucha, Aflou, Algeria. His research interests include fuzzy control, power systems, and optimization. In this study, he contributed to the controller design, the analysis of simulation results, and the preparation of the manuscript. He can be contacted at email: s.benzian@cu-aflou.edu.dz.

Hamza Sulimani is an assistant professor in the Department of Computer and Network Engineering, College of Computing, Umm Al-Qura University, Makkah, Saudi Arabia. He received his B.S. degree in electrical and computer Engineering from Umm Al-Qura University (2000), his M.S. degree in electrical and computer engineering from King Abdulaziz University (2010), and his Ph.D. degree in information technology from the University of Technology Sydney (UTS), Australia (2024). His current research interests include computer network architectures, cybersecurity, fog computing for IoT protection, and machine learning applications in network traffic analysis. He can be contacted at email: hhhsulimani@uqu.edu.sa.

Aissa Ameur received his master's and Ph.D. degrees in electrical engineering from Batna University, Algeria, in 2005 and 2012, respectively. Since 2005, he has been with the Faculty of Technology, University of Amar Telidji (Laghouat), where he is an assistant professor and a researcher at the LeDMaScD laboratory. His research interests include modeling of electrical machines, electrical drive control, fault diagnosis, artificial intelligence, and renewable energy systems. In this study, he developed the FLC, conducted the result analysis, and contributed to the manuscript preparation. He can be contacted at email: a.ameur@lagh-univ.dz.